Environ. Sci. Technol. **2010,** *44,* 150–155

Role of Nitrate in Conditioning Aquifer Sediments for Technetium Bioreduction

GARETH T. W. LAW,[†] ANDREA GEISSLER,[‡] CHRISTOPHER BOOTHMAN,[‡] IAN T. BURKE,[†] FRANCIS R. LIVENS,[‡,§] JONATHAN R. LLOYD,[‡] AND KATHERINE MORRIS*[,†,∥]

Earth System Science Institute, School of Earth and Environment, University of Leeds, Leeds, LS2 9JT, U.K., Williamson Research Centre for Molecular Environmental Science, School of Earth, Atmospheric and Environmental Sciences, The University of Manchester, Manchester, M13 9PL, U.K., and Centre for Radiochemistry Research, The University of Manchester, Manchester, M13 9PL, U.K.

Received April 9, 2009. Revised manuscript received September 30, 2009. Accepted October 26, 2009.

Here we examine the bioreduction of technetium-99 in sediment microcosm experiments with varying nitrate and carbonate concentrations added to synthetic groundwater to assess the influence of pH and nitrate on bioreduction processes. The systems studied include unamended-, carbonate buffered-, low nitrate-, and high nitrate-groundwaters. During anaerobic incubation, terminal electron accepting processes (TEAPs) in the circumneutral pH, carbonate buffered system progressed to sulfate reduction, and Tc(VII) was removed from solution during Fe(III) reduction. In the high-nitrate system, pH increased during denitrification (pH 5.5 to 7.2), then TEAPs progressed to sulfate reduction. Again, Tc(VII) removal was associated with Fe(III) reduction. In both systems, XAS confirmed reduction to hydrous $Tc(IV)O_2$ like phases on Tc removal from solution. In the unamended and low-nitrate systems, the pH remained low, Fe(III) reduction was inhibited, and Tc(VII) remained in solution. Thus, nitrate can have complex influences on the development of the metal reducing conditions required for radionuclide treatment. High nitrate concentrations stimulated denitrification and caused pH neutralization facilitating Fe(III) reduction and Tc(VII) removal; acidic, low nitrate systems showed no Fe(III)-reduction. These results have implications for Tc-cycling in contaminated environments where nitrate has been considered undesirable, but where it may enhance Fe(III)-reduction via a novel pH "conditioning" step.

Introduction

Technetium-99 is a radioactive fission product formed in nuclear reactors and is a significant radiological contaminant at nuclear facilities (*1*). It is of regulatory concern due to its long half-life ($\tau^1/_2$ 2.1×10^5 years), bioavailability, and high environmental mobility under oxic conditions. Technetium biogeochemistry in the geosphere is linked to microbially mediated terminal electron accepting processes (TEAPs) which control redox conditions. In oxic environments, Tc exists as the highly soluble pertechnetate ion ($Tc(VII)O_4^-{}_{(aq)}$) which is weakly sorbed to mineral phases and sediments. In contrast, during the development of sediment anoxia, Tc(VII) is reduced to its lower valence forms, with Tc(IV) dominating speciation as poorly soluble Tc(IV) hydrous oxide like phases (*2*). In laboratory studies, some microorganisms have been shown to reduce Tc(VII) to hydrous $Tc(IV)O_2$ enzymatically, by oxidation of electron donors such as H_2 and a restricted set of organic compounds (e.g., refs *3*−*5*). In addition, pure culture work has shown that abiotic electron-transfer reactions between Tc(VII) and biogenic Fe(II) can also facilitate reduction of Tc(VII) to poorly soluble Tc(IV) phases (*4, 6*). In the subsurface, enzymatic Tc(VII) reduction is considered ineffective, due to the rapid kinetics of Fe(II)-mediated reduction and the relatively poor recognition of low molar concentrations of the radionuclide by the hydrogenase enzymes thought to mediate enzymatic reduction (*7*). Therefore, in the majority of environmental scenarios, Tc(VII) reduction is likely dominated by abiotic reduction with Fe(II)-phases (*6, 8, 9*), although in iron-poor sediments, enzymatic reduction may be important (*8*).

As development of microbially mediated reducing conditions can reduce Tc solubility, in situ biostimulation (addition of electron donors/nutrients to sediments to promote the development of metal-reducing conditions) has been proposed as a strategy for managing Tc contamination in groundwaters (*1*). However, at nuclear facilities, subsurface conditions are often complex, with extremes in pH and high concentrations of industrial cocontaminants such as nitrate often observed (*10*−*12*). At pH ≤ 5, microbial diversity and metabolic function has been shown to be reduced at nuclear sites, critically lowering biostimulation potential (*13*−*15*). In these cases, pH neutralization via addition of base to the subsurface has been suggested as an additional remediation technique. Nitrate, which is often present at very high concentrations at nuclear facilities due to the use of nitric acid in plant operations (e.g., refs *16, 17*), can also affect biostimulation potential. High levels of nitrate reportedly hinder the development of metal-reducing conditions in sediments (e.g., refs *18, 19*); in turn, this can impact on Tc remediation as Tc(VII) reduction occurs predominantly during metal-reducing conditions (*9, 19, 20*) although in flow experiments, and one microcosm system, partial removal of TcO_4^- under nitrate reducing conditions has been reported (*10, 12, 21*).

Overcoming the inhibition of microbial communities at low-pH and understanding the influence of nitrate on bioreduction is key to understanding the potential for bioremediation to treat radionuclide contaminants within the low pH, high nitrate environments often observed at nuclear facilities. Here, we examine the biogeochemical behavior of Tc in aquifer sediments representative of the UK Sellafield nuclear facility where Tc is a groundwater contaminant (*22*). Natural, poorly buffered sediments with a low soil-pH (~5.5) were used to prepare Tc(VII) spiked microcosms, and nitrate, carbonate, and pH conditions were manipulated to examine the impact of cocontaminants on Tc biogeochemistry in aquifer sediments.

* Corresponding author phone: +44 131 343 6723; fax: +44 113 343 6716; e-mail: k.morris@leeds.ac.uk.
[†] University of Leeds.
[‡] Williamson Research Centre for Molecular Environmental Science, The University of Manchester.
[§] Centre for Radiochemistry Research, The University of Manchester.
[∥] Present address: Research Centre for Geological Disposal, School of Earth, Atmospheric, and Environmental Sciences, The University of Manchester, Oxford Rd, Manchester M13 9PL.

10.1021/es9010866

Published on Web 11/10/2009

Experimental Section

Safety. ^{99}Tc is a radioactive beta emitter (E_{max} = 294 keV). The possession and use of radioactive materials is subject to statutory controls.

Sample Collection. Sediments from the Quaternary unconsolidated alluvial flood plain deposits that underlie the Sellafield site were collected from the Calder Valley, Cumbria, during December 2006. The sampling area was located ~2 km from the Sellafield site (Lat 54°26′30 N, Long 03°28′09 W) (see Supporting Information (SI) for further details).

Bioreduction Microcosms. Sediment microcosms were prepared using a range of treatments based around a representative regional synthetic groundwater media (*23*) and with 10 mM sodium acetate added as an electron donor. Compositions were: (A) unamended-, (B) carbonate buffered-, (C) low nitrate-, and (D) high nitrate-groundwater (SI Tables 1 and 2). Groundwaters were sterilized by autoclaving (1 h at 120 °C), sparged with filtered 80/20 N_2/CO_2, and pH adjusted as required after deoxygenation. Experiments were run in triplicate. Sediment (10 ± 0.1 g) and groundwater media (100 ± 1 mL) was added to sterile 120 mL glass serum bottles (Wheaton Scientific, U.S.) using aseptic technique, the headspace was sparged with argon, and the microcosms were crimp sealed with butyl rubber stoppers. Finally, microcosms were spiked to a final concentration of 1.6 μM of TcO_4^- as ammonium pertechnetate (LEA-CERCA, France). Sterile control microcosms were established by autoclaving (3 × 20 min at 120 °C over a one-week period) and spiking with Tc. All microcosms were then incubated anaerobically at 21 °C in the dark over 250 days. Sampling of sediment slurry was conducted using sterile argon-flushed syringes and porewater and sediment samples were collected from 3 mL of slurry via centrifugation (15 000*g*, 10 min). Porewaters were sampled for total Tc, NO_3^-, NO_2^-, Fe, Mn, pH, and Eh (see below). Sediment samples were analyzed for 0.5 N HCl extractable Fe(II) and total Fe to estimate microbially produced Fe(II) ingrowth into sediments. In addition, for each sample point, 0.5 g of untreated sediment was stored under sterile conditions at −80 °C for microbiological characterization (see below). To investigate the mechanism of Tc(VII) removal in reduced sediments, additional microcosms were sterilized by autoclaving after Fe(III) reducing conditions had developed. After autoclaving, 1.6 μM of TcO_4^- was added and the sterile microcosms were equilibrated for 10 days prior to sampling as above.

Geochemical Analyses. Bulk mineralogy and sediment chemical composition were determined by X-ray diffraction (Philips PW 1050 XRD) and X-ray fluorescence (Thermo ARL 9400 XRF). Total sediment organic content was measured on a Carbo Erba EA12 (see SI). Sediment color was described using the Munsell Sediment Color Chart System (Munsell Color Company, U.S.) and sediment pH was determined (*24*). Technetium concentrations were determined by liquid scintillation counting (LSC) on a Packard Tricarb 2100TR (detection limit ~ 0.4 Bq mL^{-1}/6 nmol L^{-1}). In addition, the speciation of aqueous Tc was determined at relevant timepoints using extraction with tetraphenylarsoniumchloride (*5*). Total dissolved Fe, Mn(II), and NO_2^- concentrations were measured with standard UV−vis spectroscopy methods on a Cecil CE 3021 spectrophotometer (see SI). Aqueous NO_3^- and SO_4^{2-} were measured by ion chromatography. Total bioavailable Fe(III) and the proportion of extractable Fe(II) in the sediment was estimated by digestion of 0.1 g of sediment in 5 mL of 0.5 N HCl for 60 min, with and without hydroxylamine respectively, followed by colorimetric assay (*25*). The pH and Eh were measured with an Orion 420A digital meter and calibrated electrodes. Standards were routinely used to check the reliability of all methods and calibration regressions had $R^2 \geq 0.99$.

X-ray Absorption Spectrometry. Prereduced, Fe(II)-bearing carbonate buffered and high-nitrate amended sediment microcosms (1 g in 10 mL) were incubated with 325 μM of TcO_4^- (see SI) for 10 days. Thereafter, wet sediment was sampled under anaerobic conditions and Tc K-edge XANES and EXAFS measurements were collected at the SRS Daresbury to determine the Tc oxidation state and coordination environment. Full details of XAS methods are provided in the SI.

DNA Extraction, Ribosomal Intergenic Spacer Analysis, 16S rRNA Gene and narG Gene Analysis, And Quantitative Real-Time PCR. Microbial community DNA was extracted from sediment samples (0.2 g) using the PowerSoil DNA Isolation Kit (MO BIO Laboratories Inc., U.S.). The 16S-23S intergenic spacer region from the bacterial RNA operon was amplified from community DNA by PCR with the primers S-D-Bact-1522-b-S-20 and L-D-Bact-132-a-A-18 (*26*). Amplification was performed in a BioRad iCycler (BioRad, UK) as described by (*26*) but with 35 cycles. The amplified products were separated by electrophoresis in a 3% tris-acetate-EDTA (TAE) gel. DNA was stained with ethidium bromide and viewed under short-wave UV light using a BioRad Geldoc 2000 system (BioRad, UK).

A fragment of the 16S rRNA gene (~ 520 b.p.) was amplified by PCR from the extracted DNA of selected samples using the primers 8f and 519r (*27*). *NarG* gene fragments were amplified by PCR as described previously (*28*) using the primers na3F and narG5′R (*29*) and with an annealing temperature of 50 °C. Amplified gene fragments were cloned using the TOPO-TA Cloning system (Invitrogen, UK). A total of ~50 white colonies per sample were randomly selected and further analyzed by restriction fragment length polymorphism (RFLP) with the four-base-specific restriction endonucleases *Sau*3A and *Msp*I in parallel for 16S rRNA genes and *Hae*III and *Alu*I for *narG* genes. At least one clone of each RFLP group and all clones with a single RFLP-profile were chosen for sequencing. The gene products of the selected clones were purified by using QIAquick purification kit and directly sequenced using an ABI Prism Big Dye Terminator Cycle Sequencing Kit (PE Applied Biosystems, U.S.), following the manufacturers instructions. Sequences were obtained by using the plasmid specific primers M13f and M13r. DNA sequences were determined on an automated sequencer (ABI Prism 877 Integrated Thermal Cycler and ABI Prism 377 DNA Sequencer, Perkin-Elmer Applied Biosystems, UK). The *nar*G gene sequences were translated into amino acid sequences (www.expasy.ch). Sequences were compared with those available in the GenBank by using BLAST analysis (*30*). The possibility of chimera formation was checked by the Check_Chimera program of the RDP (*31*) and chimeras were excluded. Phylogenetic affiliation of the 16S rRNA gene sequences was estimated by BLAST and the Classifier function in RDP and the nucleotide sequences were deposited to the GenBank (see SI Tables 5−13 for accession numbers). In addition, 16S rRNA genes affiliated with the family *Geobacteraceae* were enumerated using real-time quantitative PCR using appropriate primers (GEO564F and GEO840R) (*32*) (see SI for details).

Results and Discussion

Sediment Characteristics. The sediment was dominated by quartz, sheet silicates (muscovite and chlorite), and feldspars (albite and microcline). The sediment had a high Si content (34.0 wt %) and contained Al (5.8 wt %), Fe (3.1 wt %), Ca (0.2 wt %), Na (1.0 wt %), Mg (0.5 wt %), and Mn (0.1 wt %) (SI Table 3). The air-dried sediment was red in color and ascribed a Munsell notation of 2.5YR 4/8. The sediment is best described as a uniformly graded sandy loam with an approximate particle composition of 53% sand, 42% silt, and 5% clay. The concentration of 0.5 N HCl extractable Fe(III)

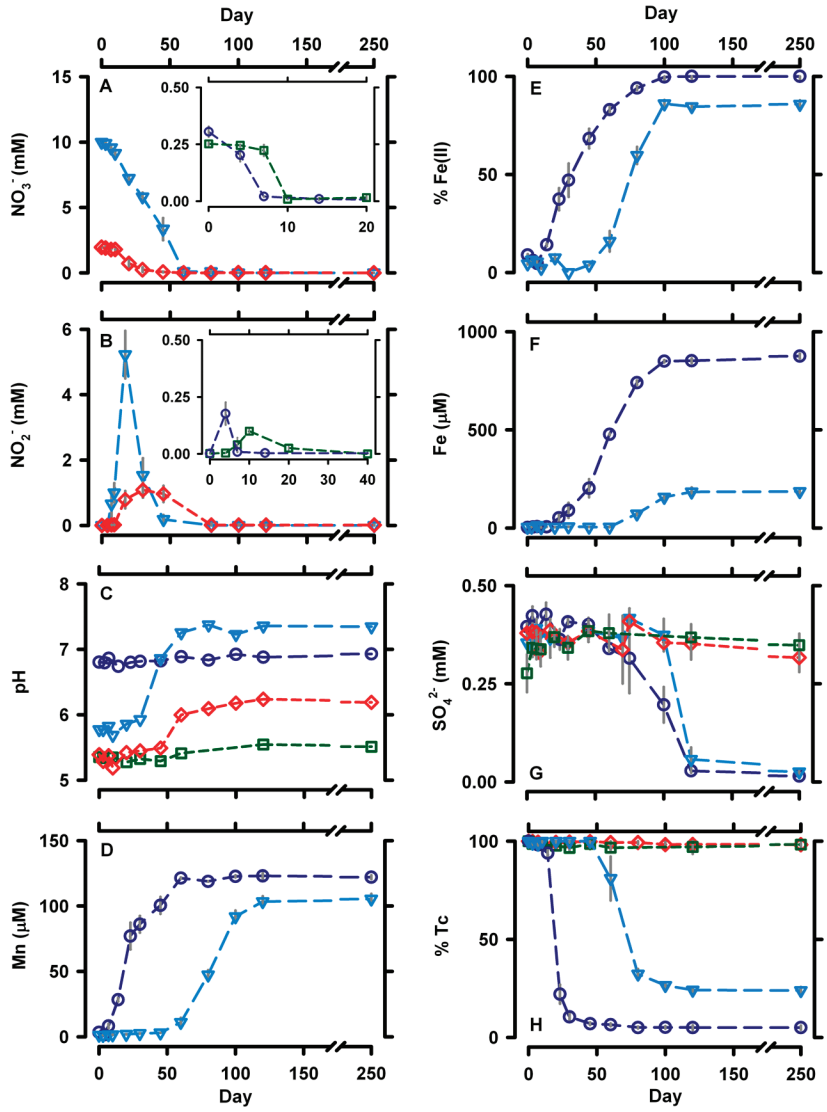

FIGURE 1. Microcosm incubation time-series data (day 0−250). (A) NO_3^-, (B) NO_2^-, (C) pH, (D) porewater Mn, (E) % extractable sedimentary Fe as Fe(II), (F) porewater Fe, (G) porewater SO_4^{2-}, and (H) % Tc remaining in solution. Note the scale break in *x*-axis. Dark blue circles = carbonate buffered system, green squares = unamended system, red diamonds = low-nitrate system, light blue inverted triangles = high-nitrate system. Error bars represent 1 σ experimental uncertainty from triplicate microcosm experiments (where not visible, error bars are within the symbol size). For clarity, Mn and Fe data showed no increase over the time course of the experiment and are not included for unamended and low-nitrate systems.

in the sediment was 8.2 ± 0.9 mmol kg^{-1}. The sediment pH was 5.5 and TOC content was 0.56 ± 0.08 wt %.

Progressive Bioreduction. Progressive bioreduction incubation experiments focused on microbially mediated TEAP progression and Tc behavior in microcosms with varying initial pH and nitrate concentrations (Figure 1; SI Table 2). An electron donor (10 mM acetate) was added to all microcosms to enhance bioreduction rates.

No biogeochemical changes were noted in sterile microcosms. In the active microcosms (Figure 1), bioreduction proceeded in all systems but at different times after experiment initiation. In the carbonate buffered system, the bioreduction process occurred almost immediately, with available nitrate (0.3 mM) completely removed from solution within 7 days (Figure 1A). In contrast, there was a lag phase before active nitrate removal in the remaining microcosms. However, after the initial lag phase, available nitrate was depleted within 10 days (unamended system), 20 days (low-nitrate system), and 60 days (high-nitrate system) (Figure 1A). In all systems, transient nitrite production (Figure 1B) occurred as active nitrate removal was observed, and the additional appearance of headspace pressure during nitrite removal indicated that denitrification proceeded to gaseous products (eqs 1−3). During this period pH increased significantly in the low-nitrate (5.5−6.2) and high-nitrate (5.5−7.2) systems (Figure 1C), which is consistent with the production of HCO_3^- and OH^- during sustained denitrification (eqs 1−3). In contrast, the pH in the unamended and carbonate buffered systems was constant, remaining at ~pH 5.5 and pH 7, respectively (Figure 1C). These results suggest that low-pH conditions do not inhibit denitrification in sediments representative of the Sellafield regional geology. Furthermore, in both the low and high-nitrate systems, denitrification generated alkalinity (eqs 1−3), with the resultant observed pH increase more pronounced in the higher nitrate system and similar to observations by past workers in mildly acidic sediments (*33, 34*). By contrast, in recent work at the radionuclide contaminated high nitrate zone of the Field Research Centre (FRC) (Oak Ridge, TN), electron donor additions to low-pH incubation experiments did not stimulate denitrification over the experimental time course unless artificial pH neutralization (via addition of crushed limestone or $NaHCO_3$) was completed (*12, 34*).

$$CH_3COO^- + 4NO_3^- \rightarrow 4NO_2^- + NaHCO_3 + CO_2 + H_2O \quad (1)$$

$$CH_3COO^- + 4NO_2^- + 2H^+ \rightarrow 2N_2O + NaHCO_3 + CO_2 + H_2O + 2OH^- \quad (2)$$

$$CH_3COO^- + 4N_2O \rightarrow 4N_2 + NaHCO_3 + CO_2 + H_2O \quad (3)$$

After denitrification, in the unamended and low-nitrate microcosms, further TEAPs did not proceed and these low-pH systems remained "poised" at constant Eh and pH, under denitrifying conditions (Figure 1A–C and SI Figure 1). In contrast, TEAP progression beyond nitrate reduction did occur in both the high-nitrate (pH 7.2 after denitrification) and carbonate (pH ~ 7.0) buffered systems. Here, manganese reduction, as indicated by Mn(II) ingrowth into porewaters, started immediately after nitrite removal in the carbonate buffered system between 4 and 7 days, and between 45 to 60 days in the high-nitrate system when pH became circumneutral as denitrification progressed (Figure 1C and D). This was followed by Fe(III)-reduction, as indicated by 0.5 N HCl extractable Fe(II) ingrowth to sediments at 7–14 days in the carbonate buffered system, and 45–60 days in the high-nitrate system. Porewater Fe was not present until ~10–20 days after the appearance of Fe(II) in the sediments (Figure 1E and F). Finally, in both systems after several months Fe(III)-reduction was largely complete and sulfate reduction began, as indicated by removal of porewater sulfate (~0.4 mM) between 120 and 250 days (Figure 1G).

Overall, the unamended and low-nitrate microcosms only progressed to denitrification even though pH adjustment (from pH 5.5 to pH 6.2) was observed in the low-nitrate system (Figure 1C). After denitrification had occurred in these two systems, no further TEAPs were observed over the time-course of the experiment. In contrast, in the high-nitrate system, denitrification led to amendment of the sediments to pH 7.2 (eqs 1–3). Further, after the initial lag period associated with pH change during denitrification, robust TEAP progression to Fe(III)- and sulfate-reduction occurred. This suggests that the metabolic activity of Fe(III)- and sulfate-reducing communities in these sediments is strongly inhibited below pH ~6.5–7.0, but that latent communities can be stimulated as the system changes to circumneutral pH. A similar pH dependence for stimulation of Fe(III) reducing bacteria has been documented at the FRC site (*13*). Here, low pH conditions inhibited the growth of Fe(III)-reducers in microcosm studies and pH neutralization was necessary to stimulate metabolic function. Interestingly, our results show that with the Sellafield type materials, microbially mediated removal of elevated levels of nitrate, a common nuclear facility cocontaminant, did occur at low pH. Furthermore, denitrification led to alkalinity generation and in turn, the associated pH change stimulated indigenous metal- and sulfate-reducing microorganisms.

Technetium Fate During Bioreduction. Tc removal occurred after denitrification, pH modification (high-nitrate system), and was commensurate with Fe(II) ingrowth into sediments (Figure 1). The presence of nitrate in microcosm porewaters has been shown to inhibit Tc(VII) reduction in other microcosm studies (e.g., refs *9, 19, 20)*, presumably because nitrate serves as a competing and more energetically favorable electron acceptor than either Fe(III) or Tc(VII). Additionally, nitrite acts as an abiotic oxidant of Fe(II), suggesting that when nitrite is present in molar excess, Fe(II) will not accumulate in sediments (*18*), and in agreement with our results (Figure 1). Indeed, the presence of excess nitrite in porewaters has been shown to inhibit the development of Fe(III) reduction and retard Tc(VII) removal in microcosm studies (*19*). Interestingly, in our sediments nitrite presence was transient and we hypothesize that denitrification proceeded to gaseous products (eqs 2 and 3) as evidenced by headspace gas pressure in our microcosms. Technetium removal was limited during the first stage of manganese ingrowth to porewaters (Figure 1D and H), consistent with the observations of other workers (*6, 9*), and robust Tc-removal occurred during active Fe(II) ingrowth to sediments. Finally, in the microbially active experiments where Tc(VII) removal had occurred, the extent of removal was different: For the carbonate buffered system, complete (99 ± 2%) removal was observed on development of Fe(III)-reducing conditions; in the high-nitrate system, only partial Tc removal (77 ± 2%) occurred even though the system proceeded to sulfate-reducing conditions. Further, in the high-nitrate system, the soluble Tc that remained under Fe(III)-reducing conditions was speciated using the TPAC extraction method (*5*) as predominantly Tc(VII) (>95% Tc(VII)), suggesting soluble Tc(IV) phases were insignificant in this system. Interestingly, the Eh in the high-nitrate system was also poised at a higher value than the carbonate system (SI Figure 1). To further assess the mechanisms of Tc removal in representative Sellafield sediments, 1.6 μM of TcO_4^- was added to prereduced carbonate buffered sediments that were sterilized during active Fe(III) reduction (~70% Fe(II) in solids). Here, 99% of added Tc(VII) was removed from solution after 10 days, indicating that Tc(VII) removal could occur via abiotic electron transfer pathways in prereduced Fe(II) bearing sediments (e.g., ref *23*).

Finally, parallel experiments were run at higher concentrations of Tc(VII) (325 μM) to allow analysis of the fate of Tc in sediments from the microcosms by XAS. Here, prereduced, microbially active Fe(III)-reducing sediment slurries from the carbonate buffered and high-nitrate systems containing >70% Fe(II) in sediments, were spiked with Tc(VII) and allowed to react for 10 days. After reaction, sediments were centrifuged and the wet sediment pellet was mounted under anaerobic conditions and analyzed by XAS (see SI for details). The k^3 weighted EXAFS and associated Fourier transforms indicate that in both samples a similar $Tc(IV)O_2$ like phase formed with diagnostic features for TcO_2 at 2.00 Å (SI Figure 2 and Table 4 (*2*)). Additional third shell fits were attempted with Tc and Fe and fitting with Tc at 2.52 Å gave a marginally better fit than Fe at 2.68 Å (SI Table 4), suggesting short-range order in the Tc(IV) precipitate.

Microbial Community Change During Bioreduction. RISA results (data not presented) were used to prescreen the bioreduction time series for microbial community change. To further analyze the extant bacterial communities, 16S rRNA gene analysis was performed on key samples from the carbonate buffered system as the incubation started (0 days) and at the end-point of Fe(III)-reduction and Tc(VII)-removal (24 days), and from the high-nitrate system as incubation started (0 days), at nitrate reduction (30 days), at the transition from denitrification to Fe(III) reduction (60 days), and at mid-Fe(III) reduction (80 days). Initially, the microbial community in both systems was diverse, with representatives of the phylum *Acidobacteria* making up ~$^1/_3$ (high-nitrate) to $^1/_2$ (carbonate buffered) of the clone libraries alongside a range of other uncultured bacteria (Figure 2; SI Tables 5 and 6). In the carbonate buffered system when Fe(III)-reduction and Tc(VII)-removal had occurred, the population consisted of 8 different phyla and with *Betaproteobacteria* dominant (Figure 2, SI Table 7). Interestingly, the sequence representing the most abundant group within the *Betaproteobacteria* was closely related (97% similarity) to an uncultured bacterium previously identified in sediments from a nuclear contamination affected field site (*20*). In addition, a close relative (97% similarity) of *Desulfosporosinus* sp. A10 was detected which is a sulfate-reducing bacteria previously detected in uranium contaminated sediments (*36*). A final 16S rRNA clone

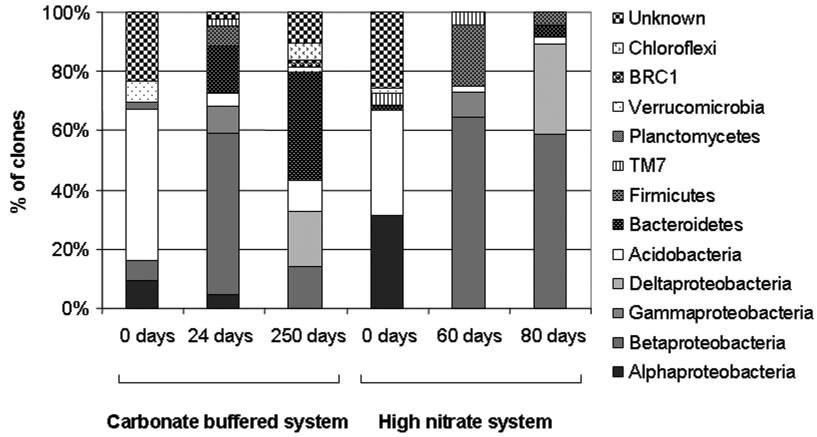

FIGURE 2. Phylum level distribution of clones from the high-nitrate and carbonate buffered systems during incubation.

library from this system at the end point of the experiment and where Fe(III)- and sulfate-reduction was complete (250 days; Figure 2; SI Table 8) was again diverse, notably with close relatives of *Geobacteraceae* present (12% of clones).

In the high-nitrate system, during denitrification (30 days), close relatives of *Betaproteobacteria* and *Firmicutes* (especially *Bacilli*) were dominant. The majority of the betaproteobacterial sequences were closely related (95% similarity) to the 16S rRNA gene sequence of *Herbaspirillum sp.* PIV-34−1, a known denitrifying bacterium (*37*) (SI Table 9). *NarG* gene analysis to target the alpha-subunit of the membrane-bound nitrate reductase was also used to further probe the molecular ecology of denitrifying organisms in this system. Most of the initial *NarG* sequences (day 0) were related to sequences retrieved from uncultured bacteria (SI Table 12). However, at 30 days a strong shift in the *NarG* gene pool was observed, with more than 60% of the *NarG* sequences distantly related to a nitrate reductase gene sequence of the genera *Bacillus* (SI Table 13). The ability of bacteria from the genera *Bacillus* to grow under anaerobic conditions using nitrate as an electron acceptor has been demonstrated previously (*38*), and our results suggest these microbes play a key role in the denitrification process in this system. At the transition from denitrification to Fe(III)-reduction and Tc(VII)-removal (60 days) (Figure 2; SI Table 10), the majority of clones were related to *Betaproteobacteria,* which are well-known denitrifiers (*39*). During Fe(III)-reduction (Figure 2, SI Table 11), *Betaproteobacteria* still represented the majority of the bacterial community (58% of clones), however, relatives of *Deltaproteobacteria* within the family *Geobacteraceae* also became significant (27%), presumably reflecting the onset of Fe(III)-reducing conditions. Fe(III)-reducing *Geobacteraceae* are widespread in aquifer environments, and the simultaneous growth of *Geobacteraceae* populations concurrent with Fe(III) reduction and removal of redox-sensitive radionuclides from solution has been observed in key biostimulation studies (*10, 40*). The increase in numbers of members of the family *Geobacteraceae* was also confirmed by the use of real-time quantitative PCR. In the high-nitrate system, genomic DNA from *Geobacteraceae* was only detected at mid Fe(III) reducing conditions (80 days) (SI Table 14). Interestingly, the concentration of *Geobacteraceae* DNA detected in this high nitrate sample was 5 times higher than that detected in the carbonate buffered system at 24 days.

Implications for Tc Biostimulation Strategies. Previous work has shown that microbial diversity and metabolic function is suppressed under low pH (*12*−*15, 35*), while robust Tc(VII) reduction is inhibited in the presence of nitrate (*9, 19, 20*). Indeed, low pH and high nitrate are often cited as potential problems in bioreduction strategies at nuclear facilities (*10, 12, 13, 15*). In this study, the metabolic function of dissimilatory metal-reducing bacteria in sediments representative of a UK nuclear site was shown to be inhibited below ~pH 6.5. In contrast, indigenous denitrifying communities where viable regardless of initial pH, and crucially, in the presence of raised levels of nitrate ($\geq$10 mmol L^{-1}), the increased activity of denitrifying microorganisms served to augment TEAP progression to Fe(III)-reduction, via nitrate removal, alkalinity generation, and pH neutralization. Further, these geochemical changes permitted the reductive removal of Tc(VII) as Tc(IV) via Fe(II) mediated abiotic electron transfer. While nitrate is generally considered a problematic cocontaminant at nuclear sites, these results suggest that its biologically facilitated removal in low-pH environments may "precondition" sediments to neutral pH, allow TEAP progression, and hence enhance radionuclide bioremediation approaches. As a consequence, the dual addition of alkaline materials and electron donors to the geosphere at some nuclear sites may be unnecessary for treatment of Tc groundwater contamination.

Acknowledgments

We thank Rob Mortimer, Lesley Neve, James Begg, and Dave Hatfield (University of Leeds), Bob Bilsborrow (SRS Daresbury), and Joyce M^{c}Beth (University of Manchester) for help in data acquisition. This work was supported by the UK Natural Environment Research Council (NERC) grants (NE/D00473X/1 and NE/D005361/1) and by a STFC beam-time award at SRS Daresbury.

Supporting Information Available

Details of sampling, spectrophotometric, XAS, and PCR methodologies; Figure 1: Eh incubation time series data; Figure 2: EXAFS and Fourier transforms; Tables 1 and 2: Synthetic groundwater media composition; Table 3: Sediment major and minor elemental composition; Table 4: EXAFS modeling; Tables 5−13: Phylogenetic affiliations of 16S rRNA gene sequences and results from the *narG* gene analysis; Table 14: Results from real-time PCR analysis using *Geobacteraceae* specific primers. This material is available free of charge via the Internet at http://pubs.acs.org.

Literature Cited

(1) Lloyd, J. R.; Renshaw, J. C. Bioremediation of radioactive waste: radionuclide microbe interactions in laboratory and field-scale studies. *Curr. Opin. Biotechnol.* **2005**, *16*, 254–260.

(2) Morris, K.; Livens, F. R.; Charnock, J. M.; Burke, I. T.; McBeth, J. M.; Begg, J. D.; Boothman, C.; Lloyd, J. R. An X-ray absorption study of the fate of technetium in reduced and reoxidised sediments and mineral phases. *Appl. Geochem.* **2008**, *23*, 603–617.

(3) Lloyd, J. R.; Nolting, H. F.; Sole, V. A.; Bosecker, K.; Macaskie, L. E. Technetium reduction and precipitation by sulfate-reducing bacteria. *Geomicrobiol. J.* **1998**, *15*, 43–56.

(4) Lloyd, J. R.; Sole, V. A.; Van Praagh, C. V. G.; Lovley, D. R. Direct and Fe(II)-mediated reduction of technetium by Fe(III)-reducing bacteria. *Appl. Environ. Microbiol.* **2000**, *66*, 3743–3749.
(5) Wildung, R. E.; Gorby, Y. A.; Krupka, K. M.; Hess, N. J.; Li, S. W.; Plymale, A. E.; McKinley, J. E.; Fredrickson, J. K. Effect of electron donor and solution chemistry on products of dissimilatory reduction of technetium by Shewanella putrefaciens. *Appl. Environ. Microbiol.* **2000**, *66*, 2451–2460.
(6) Fredrickson, J. K.; Zachara, J. M.; Kennedy, D. W.; Kukkadapu, R. K.; McKinley, J. P.; Heald, S. M.; Liu, C.; Plymale, A. E. Reduction of TcO_4^- by sediment-associated biogenic Fe(II). *Geochim. Cosmochim. Acta* **2004**, *68*, 3171–3187.
(7) Lloyd, J. R.; Thomas, G. H.; Finlay, J. A.; Cole, J. A.; Macaskie, L. E. Microbial reduction of technetium by *Escherichia coli* and *Desulfovibrio desulfuricans*: Enhancement via the use of high-activity strains and effect of process parameters. *Biotechnol. Bioeng.* **1999**, *66*, 122–130.
(8) Wildung, R. E.; Li, S. W.; Murray, C. J.; Krupka, K. M.; Xie, Y.; Hess, N. J.; Roden, E. E. Technetium reduction in sediments of a shallow aquifer exhibiting dissimilatory iron reduction potential. *FEMS Microbiol. Ecol.* **2004**, *49*, 151–162.
(9) Burke, I. T.; Boothman, C.; Lloyd, J. R.; Mortimer, R. J. G.; Livens, F. R.; Morris, K. Effects of progressive anoxia on the solubility of technetium in sediments. *Environ. Sci. Technol.* **2005**, *39*, 4109–4116.
(10) Istok, J. D.; Senko, J. M.; Krumholz, L. R.; Watson, D.; Bogle, M. A.; Peacock, A.; Chang, Y. J.; White, D. C. In situ bioreduction of technetium and uranium in a nitrate-contaminated aquifer. *Environ. Sci. Technol.* **2004**, *38*, 468–475.
(11) Singleton, M. J.; Woods, K. N.; Conrad, M. E.; DePaolo, D. J.; Dresel, P. E. Tracking sources of unsaturated zone and groundwater nitrate contamination using nitrogen and oxygen stable isotopes at the Hanford Site, WA. *Environ. Sci. Technol.* **2005**, *39*, 3563–3570.
(12) Michalsen, M. M.; Peacock, A. D.; Smithgal, A. N.; White, D. C.; Spain, A. M.; Sanchez-Rosario, Y.; Krumholz, L. R.; Kelly, S. D.; Kemner, K. M.; McKinley, J.; et al. Treatment of nitric acid-, U(VI)-, and Tc(VII)-contaminated groundwater in intermediate-scale physical models of an in-situ biobarrier. *Environ. Sci. Technol.* **2009**, *43*, 1952–1961.
(13) Petrie, L.; North, N. N.; Dollhopf, S.; Balkwill, D. L.; Kostka, J. E. Enumeration and characterization of iron(III)-reducing microbial communities from acidic subsurface sediments contaminated with uranium(VI). *Appl. Environ. Microbiol.* **2003**, *69*, 7467–7479.
(14) Reardon, C. L.; Cummings, D. E.; Petzke, L. M.; Kinsall, B. L.; Watson, D. B.; Peyton, B. M.; Geesey, G. G. Composition and diversity of microbial communities recovered from surrogate minerals incubated in an acidic uranium-contaminated aquifer. *Appl. Environ. Microbiol.* **2004**, *70*, 6037–6046.
(15) Fields, M. W.; Yan, T.; Rhee, S. K.; Carroll, S. L.; Jardine, P. M.; Watson, D. B. Impacts on microbial communities and cultivable isolates from groundwater contaminated with high levels of nitric acid-uranium waste. *FEMS Microbiol. Ecol.* **2005**, *53*, 417–428.
(16) Senko, J. M.; Mohamed, Y.; Dewers, T. A.; Krumholz, L. R. Role for Fe(III) minerals in nitrate-dependent microbial U(VI) oxidation. *Environ. Sci. Technol.* **2005**, *39*, 2529–2536.
(17) Moon, J.; Roh, Y.; Phelps, T. J.; Phillips, D. H.; Watson, D. B.; Kim, Y.; Brooks, S. C. Physicochemical and mineralogical characterization of sediment-saprolite cores from a field research site, Tennessee. *J. Env. Qual.* **2006**, *35*, 1731–1741.
(18) DiChristina, T. Effects of nitrate and nitrite on dissimilatory iron reduction by *Shewanella putrefaciens*. *J. Bacteriol.* **1992**, *174*, 1891–1896.
(19) McBeth, J. M.; Lear, G.; Morris, K.; Burke, I. T.; Livens, F. R.; Lloyd, J. R. Technetium reduction and reoxidation in aquifer sediments. *Geomicrobiol. J.* **2007**, *24*, 189–197.
(20) Li, X.; Krumholz, L. R. Influence of nitrate on microbial reduction of pertechnetate. *Environ. Sci. Technol.* **2008**, *92*, 1910–1915.
(21) Maset, E. R.; Sidhu, S. H.; Fisher, A.; Heydon, A; Worsfold, P. J.; Cartwright, A. J.; Keith-Roach, M. J. Effect of organic co-contaminants on technetium and rhenium speciation and solubility under reducing conditions. *Environ. Sci. Technol.* **2006**, *40*, 5472–5477.
(22) Nuclear Decommissioning Authority. The Sellafield environmental baseline=. 2006, http://www.nda.gov.uk/About_the_NDA-Locations-Sellafield-Sellafield_Environmental_Baseline_(1001).
(23) Wilkins, M. J.; Livens, F. R.; Vaughan, D. J.; Beadle, I.; Lloyd, J. R. The influence of microbial redox cycling on radionuclide mobility in the subsurface at a low-level radioactive waste storage site. *Geobiology* **2007**, *5*, 293–301.
(24) Thomas, G. W. Sediment pH and acidity. In *Methods of Sediment Analyses, Part 3—Chemical Methods*; Sparks, D. Ed.; Sediment Science Society of America Press: Madison 1996.
(25) Lovley, D. R.; Phillips, E. J. P. Rapid assay for microbially reducible ferric iron in aquatic sediments. *Appl. Environ. Microbiol.* **1987**, *53*, 1536–1540.
(26) Ranjard, L.; Poly, F.; Combrisson, J.; Richaume, A.; Gourbiere, F.; Thioulouse, J.; Nazaret, S. Heterogeneous cell density and genetic structure of bacterial pools associated with various soil microenvironments as determined by enumeration and DNA fingerprinting approach (RISA). *Microbial Ecol.* **2000**, *39*, 263–272.
(27) Islam, F. S.; Gault, A. G.; Boothman, C.; Polya, D. A.; Charnock, J. M.; Chatterjee, D.; Lloyd, J. R. Role of metal-reducing bacteria in arsenic release from Bengal delta sediments. *Nature* **2004**, *430*, 68–71.
(28) Geissler, A. Prokaryotic microorganisms in uranium mining waste piles and their interactions with uranium and other heavy metals. Ph.D. Dissertation, TU Bergakademie Freiberg, Freiberg, Germany, 2005.
(29) Goregues, C. M.; Michotey, V. D.; Bonin, P. C. Molecular, biochemical, and physiological approaches for understanding the ecology of denitrification. *Microb. Ecol.* **2005**, *49*, 198–208.
(30) Zhang, Z.; Schwartz, S.; Wagner, L.; Miller, W. A. greedy algorithm for aligning DNA sequences. *J. Comp. Biol.* **2000**, *7*, 203–214.
(31) Maidak, B. L.; Cole, J. R.; Lilburn, T. G.; Parker, C. T.; Saxman, P. R.; Stredwickm, J. M.; Garrity, G. M.; Li, B.; Olsen, G. J.; Pramanik, S.; et al. The RDP (Ribosomal Database Project) continues. *Nucleic Acids Res.* **2000**, *28*, 173–174.
(32) Cummings, D. E.; Snoeyenbos-West, O. L.; Newby, D. T.; Niggemyer, A. M.; Lovley, D. R.; Achenbach, L. A.; Rosenzweig, R. F. Diversity of *Geobacteraceae* species inhabiting metal-polluted freshwater lake sediments ascertained by 16S rDNA analyses. *Microbial Ecol.*, **2003**, *46*, 257–269.
(33) Postma, D.; Boesen, C.; Kristiansen, H; Larsen, F. Nitrate reduction in an unconfined sandy aquifer: water chemistry, reduction processes and geochemical modeling. *Water Resour. Res.* **1991**, *27*, 2027–2045.
(34) Baeseman, J. L.; Smith, R. C.; Silverstein, J. Denitrification potential in stream sediments impacted by acid mine drainage: Effects of pH, various electron donors, and iron. *Microb. Ecol.* **2006**, *51*, 232–241.
(35) Edwards, L.; Kusel, K.; Drake, H.; Kostka, J. E. Electron flow in acidic subsurface sediments co-contaminated with nitrate and uranium. *Geochim. Cosmochim. Acta* **2007**, *71*, 643–654.
(36) Nevin, K. P.; Finneran, K. T.; Lovley, D. R. Microorganisms associated with uranium bioremediation in a high-salinity subsurface sediment. *Appl. Environ. Microbiol.* **2003**, *69*, 3672–3675.
(37) Probian, C.; Wülfing, A.; Harder, J. Anaerobic mineralization of quaternary carbon atoms: Isolation of denitrifying bacteria on pivalic acid (2,2-dimethylpropionic acid). *Appl. Environ. Microbiol.* **2003**, *69*, 1866–1870.
(38) Hoffmann, T.; Troup, B.; Szabo, A.; Hungerer, C.; Jahn, D. The anaerobic life of *Bacillus subtilis*: Cloning of the genes encoding the respiratory nitrate reductase system. *FEMS Microbiol. Lett.* **1995**, *131*, 219–225.
(39) Akob, D. M.; Mills, H. J.; Kostka, J. E. Metabolically active microbial communities in uranium-contaminated subsurface sediments. *FEMS Microbiol. Ecol.* **2007**, *59*, 95–107.
(40) Holmes, D. E.; Finneran, K. T.; O'Neil, R. A.; Lovley, D. R. Enrichment of members of the family *Geobacteraceae* associated with stimulation of dissimilatory metal reduction in uranium contaminated aquifer sediments. *Appl. Environ. Microbiol.* **2002**, 2300–2306.

ES9010866